Resuscitation 133 (2018) 124–136

Contents lists available at ScienceDirect

Resuscitation

journal homepage: www.elsevier.com/locate/resuscitation

Review

Brain imaging in comatose survivors of cardiac arrest: Pathophysiological correlates and prognostic properties

H.M. Keijzer[a,b,c,*], C.W.E. Hoedemaekers[b], F.J.A. Meijer[d], B.A.R. Tonino[e], C.J.M. Klijn[c], J. Hofmeijer[a,f]

[a] Department of Neurology, Rijnstate Hospital, Arnhem, the Netherlands
[b] Department of Intensive Care Medicine, Radboud University Medical Centre, Nijmegen, the Netherlands
[c] Department of Neurology, Donders Institute for Brain, Cognition, and Behaviour, Radboud University Medical Centre, Nijmegen, the Netherlands
[d] Department of Radiology and Nuclear medicine, Radboud University Medical Centre, Nijmegen, the Netherlands
[e] Department of Radiology, Rijnstate Hospital Arnhem, the Netherlands
[f] Department of Clinical Neurophysiology, University of Twente, Enschede, the Netherlands

ARTICLE INFO

Keywords:
Hypoxic-ischemic brain injury
Cardiac arrest
Neuroimaging
Prognosis

ABSTRACT

Introduction: Hypoxic-ischemic brain injury is the main cause of death and disability of comatose patients after cardiac arrest. Early and reliable prognostication is challenging. Common prognostic tools include clinical neurological examination and electrophysiological measures. Brain imaging is well established for diagnosis of focal cerebral ischemia but has so far not found worldwide application in this patient group.

Objective: To review the value of Computed Tomography (CT), Magnetic Resonance Imaging (MRI), and Positron Emission Tomography (PET) for early prediction of neurological outcome of comatose survivors of cardiac arrest.

Methods: A literature search was performed to identify publications on CT, MRI or PET in comatose patients after cardiac arrest.

Results: We included evidence from 51 articles, 21 on CT, 27 on MRI, 1 on CT and MRI, and 2 on PET imaging. Studies varied regarding timing of measurements, choice of determinants, and cut-off values predicting poor outcome. Most studies were small (n = 6–398) and retrospective (60%). In general, cytotoxic oedema, defined by a grey-white matter ratio < 1.10, derived from CT, or MRI-diffusion weighted imaging < 650×10^{-6} mm^2/s in > 10% of the brain could differentiate between patients with favourable and unfavourable outcomes on a group level within 1–3 days after cardiac arrest. Advanced imaging techniques such as functional MRI or diffusion tensor imaging show promising results, but need further evaluation.

Conclusion: CT derived grey-white matter ratio and MRI based measures of diffusivity and connectivity hold promise to improve outcome prediction after cardiac arrest. Prospective validation studies in a multivariable approach are needed to determine the additional value for the individual patient.

Introduction

Most patients surviving cardiac arrest remain comatose immediately after the circulation has been restored, as a result of transient diffuse cerebral ischemia [1]. Of these patients 30–70% never regain consciousness as a result of severe hypoxic-ischemic brain injury [1–5]. Hypoxic-ischemic brain injury is the main cause of death or disability in patients who survive to hospital admission. Early identification of the severity of brain damage and prediction of subsequent outcome is challenging. Brain imaging by computed tomography (CT) or magnetic resonance imaging (MRI) is well established for diagnosis of focal cerebral ischemia [6] but has so far not found worldwide clinical application in this patient group [7].

Diagnosis and prognosis of comatose patients after cardiac arrest is generally based on neurological examination and electrophysiological measures [8–10]. Absence of pupillary and corneal

* Corresponding author at. Rijnstate Hospital, department of Neurology, P.O. box 9555, 6800 TA, Arnhem, the Netherlands.
E-mail address: HMKeijzer@rijnstate.nl (H.M. Keijzer).

https://doi.org/10.1016/j.resuscitation.2018.09.012
Received 11 July 2018; Received in revised form 12 September 2018; Accepted 14 September 2018

reflexes, absence of the N20 response of Somatosensory Evoked Potentials (SSEP) [9], and lasting isoelectric or low voltage EEG patterns 24 h after cardiac arrest are almost invariably associated with a poor outcome [11]. The post resuscitation guidelines from the European Resuscitation Council also consider absence of EEG reactivity and high serum Neuron Specific Enolase levels as predictors of poor outcome, although not 100% specific [5,9]. Together, neurological examination and electrophysiological measures allow reliable prediction of good or poor outcome in 50% of patients [2,11]. In the remaining 50% of patients after cardiac arrest who are comatose and treated in intensive care units, we are unsure of the severity of their brain damage and unsure of what we can tell their relatives regarding the chances of recovery.

Improved prognostication of patients who are comatose after cardiac arrest may add to communication between doctors and families and support treatment decisions. This applies to support for treatment continuation in those with a chance of recovery, and for discontinuation in the absence of relevant recovery perspectives. Here we review the pathophysiology of hypoxic ischemic brain injury and build on pathophysiological principles to discuss the applicability of four imaging techniques of the brain: Computed Tomography (CT), Magnetic Resonance Imaging (MRI), Positron Emission Tomography (PET) and Single Photon Emission CT (SPECT). In addition, we summarize the evidence of the diagnostic and prognostic accuracy of these imaging modalities in comatose patients after cardiac arrest.

Literature search

For analysis of the evidence of imaging measures, we applied a search in the Medline and PubMed databases from 2000 to May 2018. We used combinations of the following words and MeSH terms: “post-anoxic encephalopathy”, “hypoxic coma”, “cardiopulmonary resuscitation”, “cardiac arrest”, “MRI”, “CT”, “PET”, “SPECT”, “outcome” and “prognosis”. We screened articles for eligibility based on the abstracts. We excluded review articles, case studies, studies in paediatric populations, or animal studies. Studies before 2000 were excluded to prevent inclusion of studies using older, less precise imaging techniques.

Of articles on studies on the diagnostic or prognostic accuracy of CT, MRI, PET, or SPECT, we extracted the diagnostic determinants that were used, including cut off values if applicable, and the primary outcome measure.

Results

In our review, we included 51studies of which 21 on CT (Table 1), 27 on MRI (Table 2),1 using both CT and MRI, and 2 using PET (Table 3). We found no studies on the diagnostic or prognostic value of SPECT. Since diagnostic criteria and study designs were disparate, it was not possible to meta-analyse any results. Studies were generally small (6–398 patients), leading to wide confidence intervals (imprecision), often retrospective (60%), and cut off values were most often not predefined, leading to a considerable risk of bias.

Pathophysiological considerations

The human brain represents 2% of the body weight and accounts for 20% of oxygen consumption and 25% of glucose utilization [12,13]. Insufficient blood flow to the brain leads to loss of neuronal function and viability, sequentially. Transitions from reversible to irreversible neuronal damage occur on timescales ranging from minutes to hours and probably even days [14], depending on the remaining blood flow, the duration of ischemia and the extent of (delayed) reperfusion (Fig. 1) [15].

Changes in synaptic functioning (i.e. the process in which neurons pass chemical signals to other neurons) are the earliest consequence of cerebral ischemia and may occur within seconds, even at moderately reduced perfusion levels. Early synaptic failure results from presynaptic damage with impaired transmitter release [16]. Disappearance of synaptic activity may be reversible. However, without timely recovery of cerebral perfusion, disturbances of synaptic transmission may become permanent, with preserved membrane potential [17]. Synaptic damage goes along with disturbed EEG patterns or evoked potentials [2], but cannot be visualized with conventional imaging techniques.

Lower perfusion levels of lead to malfunctioning of energy dependent ion pumps, especially ATP dependent sodium-potassium pumps in the neuronal and glial plasma membrane [18]. Malfunctioning of these pumps causes loss of ion gradients across the plasma membrane (depolarization) and inability to generate action potentials. With failure of transmembrane sodium-potassium pumps, the net inflow of osmotically active particles (sodium, chloride) is larger than the outflow (potassium). This causes an increased intracellular osmolality [19]. Subsequent inflow of water leads to cytotoxic (intracellular) oedema: swelling of neuronal and glial cells and a decrease of the extracellular compartment, which may be visualized with CT or diffusion weighted MRI [20]. Disruption of the blood brain barrier, together with accumulation of osmotically active substances, leads to vasogenic (extracellular) oedema, visible on CT and T2 weighted or FLAR MRI [20]. With cytotoxic oedema, the total tissue brain mass will initially remain unchanged. Vasogenic oedema leads to tissue swelling, tissue shifts, and eventually a rise in intracranial pressure, since a new constituent (water from the vascular space) is added.

Apart from strictly neurophysiological responses, cerebral ischemia and reperfusion may lead to additional brain injury through complex series of events, including excitotoxicity, inflammation, and microvascular damage [21].

Neuronal damage may selectively affect specific areas of the brain, with grey matter (GM) being more vulnerable than white matter (WM), and hippocampus, cerebellar Purkinje cells, pyramidal cells in the neocortex, and parts of thalamus and striatum more vulnerable than other areas [21,22]. Also, excitatory synapses are probably more vulnerable than inhibitory synapses, leading to disturbed excitation-inhibition ratio’s that are associated with characteristic EEG patterns and myoclonic status [23,24].

Neuroimaging techniques in relation to pathophysiological mechanisms

Computed tomography (CT)

CT allows for investigation of both cytotoxic and vasogenic oedema, and mass effects of the brain. Cytotoxic oedema first decreases the tissue density of cerebral grey matter and later also of white matter. In the reviewed studies, this is measured as an absolute decrease, an absolute difference, or the ratio between grey matter and white matter

density. The 'Loss of Boundary' sign is a qualitative measure expressing decreased distinctive value between grey and white matter. The grey-white matter ratio (GWR) quantifies this. The GWR is calculated as the ratio of Hounsfield Units (HU) between grey and white matter, and is the most studied CT parameter.

Mass effects can become visible as the 'sulcal effacement sign' (resulting from displacement of cerebrospinal fluid in sulci, Fig. 2) or the 'pseudo subarachnoid haemorrhage sign' (p-SAH, high attenuation along cisterns and sulci resulting from distension of superficial veins). An increased Optic Nerve Sheath Diameter (ONSD) is an indicator of elevated intracranial pressure [25]. Literature suggests that an ONSD > 5 mm corresponds to intracranial pressure > 20 cmH_2O [25].

Changes in grey matter attenuation, p-SAH and mass effects are all time dependent. Decreased grey matter attenuation and increased ONSD can be measured within hours after cardiac arrest [26–30]. Sulcal effacement and the loss of boundary sign can be seen as early as 1 h after cardiac arrest, although very subtle in this early phase [29]. P-SAH has a prolonged detection period, from hours after the event up to 59 days [31,32], when other prognostic parameters might already have returned to normal values [32].

Magnetic resonance imaging (MRI)

MRI Diffusion Weighted Imaging (DWI) detects diffusion of water molecules and is sensitive to detection of cytotoxic oedema, which reduces diffusivity. MRI Fluid Attenuation Inversion Recovery (FLAIR) employs on the water content of tissue, but discards the influence of the cerebrospinal fluid. Therefore, MRI-FLAIR is sensitive to detection of cytotoxic and vasogenic cerebral oedema. With both sequences, abnormalities become apparent as signal hyperintensities (Fig. 3). Cerebral oedema arises within hours after cardiac arrest and is most prominent after approximately 3 days [33,34]. In this early phase, restricted diffusion can be found using DWI [33,34]. DWI abnormalities classically start to disappear after 7–10 days [35,36]. Increased signal intensity on FLAIR images becomes visible after 1–2 days and remains visible up to weeks after disappearance of DWI abnormalities [33]. This represents vasogenic oedema in the early phase, and indicates gliosis when it remains visible for weeks or longer.

Restricted diffusion by cytotoxic oedema can be quantified by calculating the Apparent Diffusion Coefficient (ADC) value of each voxel. There is no unanimity regarding normal boundaries, but rough indications for normal values in the brain are white matter: 670–800 $*10^{-6}\,mm^2/s$ and grey matter: 700–1000 $*10^{-6}\,mm^2/s$ [37]. A decrease in ADC value indicates the presence of cytotoxic oedema [20]. Of note, these values depend on the chosen protocol settings, such as b-values and the magnetic field strength. ADC values also correct for hyperintensities on DWI that are not caused by restricted diffusion, but by high T2 values influencing the DWI signal. This is called the "T2 shine through effect".

Relatively new MRI techniques allow for analysis of connectivity in the brain. These techniques are not yet implemented in clinical practice. Only a small number of studies has been performed in this field.

Functional MRI (fMRI) estimates brain activity through changes in blood flow by means of the Blood Oxygen Level Dependend (BOLD) signal. Subsequent connectivity analyses are based on synchronous activity in different parts of the brain. The brain in rest shows synchronous activity in various specific brain areas, known as the resting state networks. Examples are the Default Mode Network, the executive control network, the Salience Network, the sensorymotor network, and the auditory and visual network [38].

Structural connectivity can be estimated by means of Diffusion Tensor Imaging (DTI). DTI is an advanced variation of DWI, taking into account the direction of diffusion of water molecules. The random motion of water molecules is restricted by the normal architecture of neuroglial tissue and fiber tracts, which is called anisotropy. Fractional anisotropy is a quantitative DTI based measure for the degree of anisotropy Anisotropic structures, such as white matter tracts, have high fractional anisotropy.

Positron emission tomography (PET)

PET imaging is based on glucose or oxygen metabolism. This is measured indirectly by the blood flow towards different parts of the brain. Both the cerebral blood flow and the metabolism of the brain are of interest in hypoxic-ischemic brain injury. These are measured by 5 relevant PET parameters: cerebral blood flow, oxygen metabolism ($CMRO_2$), oxygen extraction fraction, cerebral blood volume and glucose consumption. Hypoxic brain damage eventually leads to a decrease in all these parameters, because of the decreased neuronal activity, disturbed cerebral autoregulation and microvascular dysfunction.

Prognostic value of neuroimaging techniques

Computed tomography

Decreased attenuation of grey matter

Patients precluding cerebral recovery show lower HU values in the grey matter than patients with favourable outcome [39]. An absolute decrease of tissue density in the grey matter attenuation alone is an unreliable predictor of poor outcome [40,41]. The predictive value increases when attenuation measures of grey and white matter are related, for example as expressed by the grey white matter ratio (GWR). We included 17 studies that studied GWR as a predictor (n = 25–283). GWR values as a single prognosticator predicted poor outcome with 100% specificity and varying sensitivity (5.6%–55%) [26–28,40–53]. Differences are explained by variable definitions of poor outcome, variable time-periods between the arrest and CT, a variation in regions of interest (ROIs) that were investigated, accuracies of ROI selection (manual or automated) [27,41], differences in technical details of the CT scanner, scanning protocols, and in reconstruction algorithms.

Other attenuation based parameters than GWR that have been investigated to predict poor outcome are: I. An absolute difference in HU values between cortex and white matter of < 5 (specificity of 100%, sensitivity of 63%) [30]. II. The sulcal effacement sign (specificity of 100%, sensitivity of 14.4–56.6%) [29,54]. III. The Loss of Boundary sign at the level of the basal ganglia (specificity of 92%, sensitivity of 81%) [29]. The loss of boundary sign was qualitatively obtained, with an inter-observer concordance of 76% between two trained radiologists. The authors gave no clear definitions of this sign.

Table 1
CT parameters and their prognostic values.

Source	Study design	n	Region of interest		Median time ROSC to scan	Cut off value	Sens (95%CI)	Spec (95%CI)	Definition of poor outcome
			GM structures	**WM structures**					
Grey-White matter Ratio									
Torbey et al. [45]	Retrospective	25	Caudate nucleus	Internal capsule	< 48hr	1.18	36	100	Death
Metter et al. [40]	Retrospective	240	Caudate nucleus Putamen Thalamus Cortex	Internal capsule Corpus callosum Centrum semiovale	4.2hr	1.20	36	98	Death
Lee et al. [44]	Retrospective	224	Putamen	Corpus callosum	96.5 min	1.17	52.9	100	CPC 3–5 at discharge
Scheel et al. [43]	Retrospective	98	Putamen Thalamus Medial Cortex	Internal capsule Corpus callosum Medial WM	5hr	1.16	38	100	CPC 3–5 at discharge
Cristia et al. [27]	Retrospective	77	–	–	157min	1.10	13-19	96-100	CPC 3–5 at discharge
Hwan Kim et al. [42]	Retrospective	91	Caudate nucleus Putamen	Corpus callosum Internal capsule	56 min	1.23	83.8 (73–92)[a]	100	CPC 3–5 at discharge
Gentsch et al. [28]	Retrospective	98	Putamen	Internal capsule	5hr	1.11	44.3	100	CPC 3–5 at discharge
Chae et al. [26]	Retrospective	119	Putamen High cortical level	Internal capsule Corpus callosum Centrum semiovale	1hr	1.13	20.3	100	CPC 3–5 at 1 month
Lee et al. [41]	Retrospective	164	Putamen	Corpus callosum	67 min	1.20	43.5	100	CPC 3–5 at discharge
Wu et al. [46]	Prospective	151	Putamen	Internal capsule	< 72hr	–	8 (4–16)	100 (73–100)	mRS > 4 at 6 months
Sahutoglu et al. [47]	Retrospective	100	Caudate nucleus	Internal capsule	< 72hr	1.18	54.9[b]	100	Death
Scarpino et al. [48]	Retrospective	183	Caudate nucleus, putamen	Internal capsule, corpus callosum	< 24hr	1.21	41,7 (33.6–50.2)	100 (94–100)	CPC 4–5 at 6 months
Youn et al. [49]	Retrospective	240	Caudate nucleus, putamen, medial cortex	Corpus callosum, internal capsule, medial WM.	< 24hr	1.077	15.6 (11–21.1)	100 (84.6–100)	CPC 3–5 at discharge
Jeon et al. [50]	Retrospective	39	Caudate nucleus, Putamen, Thalamus	Corpus callosum, Internal capsule	90 min	1.21	75,8(57,7–88,9)	100 (54,1–100)	CPC 3–5 at discharge
Lee et al. [51]	Retrospective	283	Putamen	Corpus callosum	~50 min	1.107	5.6	100	CPC 3–5 at discharge
Choi et al. [52]	Retrospective	28	Caudate nucleus, Putamen	Corpus callosum, Internal capsule	3.9hr	1.22	63	100	GOS 1–2 at discharge
Torby et al. [53]	Retrospective	32	Caudate nucleus	Internal capsule	< 48hr	1.18	83[a]	100	GOS 1–3 at discharge
Other attenuation measures									
Presence of LOB sign									
Inamasu et al. [29]	Retrospective	75	Qualitative LOB sign at the level of the basal ganglia		50 min	LOB sign present	81	92	CPC 3–5 at 6 months
Presence of sulcal effacement sign/ generalized cerebral oedema									
Inamasu et al. [29]	Retrospective	75	Sulcal effacement sign at the level of the centrum semiovale		50 min	Sulcal effacement sign present	32	100	CPC 3–5 at 6 months
Moseby-Knappe et al (2017)	Post-hoc analysis	357	Whole brain		1: < 24hr 2: d 1-7	Generalized cerebral oedema	1;14.4 2:56.6	100	CPC 3–5 at 6 months
Difference between GM and WM HU values									

(*continued on next page*)

Table 1 (*continued*)

Source	Study design	n	Region of interest		Median time ROSC to scan	Cut off value	Sens (95%CI)	Spec (95%CI)	Definition of poor outcome
			GM structures	WM structures					
Yamamura et al. [30]	Retrospective	58	Cerebral cortex Caudate nucleus Putamen	Subcortical WM Internal capsule Corpus callosum	–	GM-WM < 5.5	63	100	GOS 1–2 at discharge
Other CT measures									
Pseudo sub-arachnoid haemorrhage sign									
Yuzawa et al. [32]	Retrospective	45	Cisterns, sulci, ventricles, parenchyma		–	p-SAH present	31	100	MRs 4–6 (timing unknown)
Lee et al. [31]	Retrospective	398	Basal cisterns or sulci, subarachnoid and intracranial areas		39.5 min	p-SAH present	11.5 (8.1–16.0)	100 (96.1–100)	CPC 3–5 at discharge
Optic Nerve Sheath diameter									
Hwan Kim et al. [42]	Retrospective	91	Optic nerve		56 min	> 6.21 mm	55.9 (43.3–67.9)	100	CPC 3–5 at discharge
Chae et al. [26]	Retrospective	119	Optic nerve		1hr	> 7.0mm	5.5	100	CPC 3–5 at 1 month

GM: grey matter, WM: white matter, Sens: sensitivity, Spec: specificity, CPC: cerebral performance category, HU: Hounsfield unit, GOS: Glasgow outcome scale, LOB: loss of boundary, NS: not specified. HC: healthy controls, MRs: modified Ranking scale. Min: minutes, n: number of included PAE patients.
When studies investigated multiple ROI's, the ROI's with the best results are given.
Confidence intervals are only displayed if mentioned by the authors.
[a] This study analysed a predictive model combining GWR with Glasgow coma Scale and time to return of circulation as predictors.
[b] The authors of this study gave no sensitivity value. This value is calculated using the data provided in the article.

Pseudo sub-arachnoid haemorrhage sign

Approximately 8–20% of the patients show p-SAH, based on 2 studies (n = 45–398) [31,32]. The presence of p-SAH predicted poor outcome with specificities of 100% and sensitivities of 30% [32] and 11.5% [31] when measured within one hour after cardiac arrest.

Optic nerve sheath diameter

Two studies (n = 91–119) reported significantly higher ONSD in patients with poor as compared with good outcome, measured by CT within 24 h [26,42]. Slightly different cut-off values predicting poor outcome with a specificity of 100% were reported: ONSD > 7 mm (sens 5.5%) [26], and ONSD > 6.21 mm (sens 55.9%) [42]. Combining ONSD with GWR resulted in a multivariable predictive model with a specificity of 100% and a sensitivity of 92.6% [42].

Magnetic resonance imaging

Qualitative DWI and FLAIR

We included thirteen studies on qualitative scoring of DWI and FLAIR scans in patients with hypoxic-ischemic brain injury (n = 10–172) [33–36,50,55–59], measured between 1 and 150 days post cardiac arrest. All studies found signal abnormalities in the cortex and deep grey matter [33–36,55,56]. The cerebellum and hippocampus were involved in four of these studies [33,35,55,56]. The subcortical white matter and corpus callosum showed the least signal abnormalities. Predictive values for poor outcome of qualitative interpretation of DWI and FLAIR scans are reported by 3 studies, with sensitivities ranging between 78.8–98.5% en specificities of 46.2–100% [50,59,60]. Treatment with hypothermia did not influence DWI and FLAIR results [34,36].

Four prospective studies (n = 19–68) used a semi-quantitative approach by a standardized scoring system [34,36,61,62]. DWI and FLAIR scans were scored by trained radiologists, according to the degree of abnormality on a scale from 0 to 4 in regions of the cortex and deep grey nuclei. They found significantly more signal abnormalities in patients with unfavourable outcomes [34,36,61]. This difference remained significant from the first day up to two weeks after the arrest [34,36,61]. Signal abnormalities found in the cortex and deep grey nuclei predicted poor outcome with 100% specificity and sensitivities of 66% (cortex score > 27 (max. 88)) [36], 40% (whole brain score ≥41 (max. 168)) [62], and 100% (cut-off value not specified) [34].

ADC

We included ten studies on ADC values, obtained from DWI scans (n = 9–125). Decreased ADC values, most often seen in the cortex and basal ganglia, were associated with poor outcome [55,57,63–69]. ADC values < 650 to 700 $*10^{-6}$ mm^2/s in minimally 10–22% of the brain volume predicted poor outcome with a specificity of 100% and sensitivities ranging from 41% to 81% [55,63,65,66]. The optimal time window to perform ADC imaging to predict poor outcome was between day two and five after cardiac arrest [55,65]. No ADC lesions could be found within the first hours after arrest [67]. One study reported no significant differences in ADC values between patients with poor and good outcome [70].

fMRI

Three studies investigated the within and between network connectivity of resting state networks using fMRI at 3–13 days after cardiac arrest (n = 12–47). Patients with poor outcome typically showed decreased [61,71] or disrupted [72] network strengths in default mode network, including the precuneus, posterior cingulate cortex, mesiofrontal and anterior cingulate cortex, and temporoparietal junction areas. The connectivity between the default mode network and the Salience Network showed the highest discriminative value between patients with poor versus good outcome on a group level

Table 2
MRI parameters and their prognostic values.

Source	Study design	n	Region of Interest	Median time ROSC-Scan	Cut off-value	Sens (95% CI)	Spec (95%CI)	Definition poor outcome	Main results
Qualitative DWI and FLAIR[a]									
Wijdicks et al. [33], Els et al. [86], Topcuoglu et al. [60] Park et al. [34], Howard et al. [35], Greer et al. [59], Hirsch et al. [36], Mlynash et al. [55], Ryoo et al. [56], Youn et al. [57], Leao et al. [58], Jeon et al. [50], Velly et al. [62]	Prospective: 7, Retrospective: 6	10–172	Whole brain	1-150 days		78,8-98.5	46.2-100 –		Qualitative scoring of FLAR and DWI scans reveal that the cortex and deep grey matter tissues are most affected by PAE. DWI abnormalities become visible within hours after the arrest and disappear after a week. FLAIR abnormalities appear after a few days and remain visible up to weeks. MRI lesions are associated with poor neurological outcome, although patients with good neurological outcome often show mild to moderate abnormalities in the GM. Only 3 studies reported predictive values of visual DWI and/or FLAIR analysis.
FLARI-DWI Cortex Score / Cortex and deep grey nuclei score[b]									
Hirsh et al. [36]	Prospective	68	Cortex + deep grey nuclei	77hr	Cortex score > 27	66 (47–81)	100(88–100)	GOS 1–2	The cortex score, the deep grey nuclei score and the overall score of DWI and FLAIR all predicted poor outcome. The cortex score is the most practical one to use.
Park et al. [34]	Prospective	19	Cortex + deep grey nuclei	121 min	–	100 (73.5–100)	100(59–100)	CPC 3–5	The cortex score and the cortex + deep grey nuclei score and the overall score of DWI best predicted poor outcome. The cortex plus deep grey nuclei score is considered the most practical.
Sair et al. [61]	Prospective	46	Cortex + deep grey nuclei	12.6 days	–	–	–	CPC 3–5 at 12 months	Patient with unfavourable outcome displayed a significantly increased cortex score.
Velly et al. [62]	Prospective	200	Whole brain	13 days	Whole brain DWI-FLAIR score ≥41	40(31–50)	100(89–100)	Best achieved CPC score of 3–5 in the first 6 months.	The whole brain DWI-FLAIR score was significantly higher in patients with poor outcome. Sensitivity is slightly lower when using the cortex plus deep grey nuclei score (sens. 37%)
ADC									
Mlynash et al. [55]	Prospective	33	Whole brain	80hr	ADC < 650×10^{-6} mm^2/ s in 10% of the brain within 49-108hr after CA	–	100	CPC 3–6 at 6 months	Patients with good outcome showed increased diffusivity, while poor outcome patients showed decreased diffusivity when compared to healthy controls. Affected neuronal structures reached their nadir between 3–5 days.
Hirsch et al. [63]	Retrospective	125	Whole brain	69hr	ADC < 650×10^{-6} mm^2/ s in 22% of the brain	52	100	failure to regain consciousness within 14 days and/or death during hospitalization	Decreased ADC values are an independent predictor of poor outcome.

(*continued on next page*)

Table 2 (*continued*)

Source	Study design	n	Region of Interest	Median time ROSC-Scan	Cut off-value	Sens (95% CI)	Spec (95%CI)	Definition poor outcome	Main results
Kim et al. [64]	Retrospective	110	Whole brain	53hr	The biggest cluster with ADC < 560×10^{-6} mm^2/s. Cluster size not specified	89,2	100	CPC3–5 at 6 months	Low ADC values indicate poor outcome. The DC-LADCV was the best predictor of poor outcome.
Mettenburg et al. [70]	Retrospective	33	Whole brain	–	ADC < 700×10^{-6} mm^2/s.	–	–	Death, persistent VS or admission to a nursing home at discharge.	Regional hippocampal or basal ganglia injury was associated with poor outcome. EEG and MRI measures appear to complement each other. Patients with malignant EEG patterns showed less structural brain injury based on MRI, although they still had a poor outcome.
Wijman et al. [65]	Prospective	51	Whole brain	88hr	ADC < 650×10^{-6} mm^2/s in 10% of the brain within 49-108hr after CA	81	100	Death at 6 months and absent pupillary reflexes or SSEP at 72 h or VS at 1 month	DWI between 49-108 h after arrest best differentiates between patient with favourable and unfavourable outcome. Thresholds of ADC < 400-450 $\times 10^{-6}$ mm^2/s could differentiate between patients who regained an independent lifestyle and patients who remained severely disabled.
Wu et al. [66]	Retrospective	80	Whole brain	2 days	Median whole brain ADC < 665×10^{-6} mm^2/s	41 (29–54)	100 (73–100)	MRs > 3 at 6 months	Patients with poor outcome display significantly decreased ADC values compared to patient with favourable outcome. Timing of the scan and selection of brain regions are influencers of the measured differences between patient groups.
Youn et al. [57]	Retrospective	22	Whole brain	1st: 6hr 2nd: 74hr	–	–	–	CPC 3–5 at discharge	DWI and ADC values have a temporal profile that is different according to anatomic regions. The DWI after 48 h is a better predictor of outcome than the early scan.
Kim et al. [68]	Retrospective	43	Occipital lobe	< 72 h	ADC < 616×10^{-6} mm^2/s	90.6	100	CPC 3–5 at 6 months	The occipital lobe showed the highest predictive value. This cut-off value could identify additional poor outcome patients with normal NSE values.
Choi et al. [69]	Prospective	22	Putamen	53 hr	ADC < 750×10^{-6} mm^2/s	93 (66–100)	100 (56–100)	GOS 1–3 at 3 months	Most ADC damage is found in basal ganglia and cortex, with the ADC value in the Putamen leading to the highest sensitivity. ADC values of patients with good outcome are comparable to healthy controls.
Heradstveit et al. [67]	Prospective	10	Centrum semi-ovale, lentiform nucleus cerebellum & visual ischemic lesions	1st: 2 h 2nd: 24 h 3rd: 96 h	ADC < 600×10^{-6} mm^2/s	–	–	Survival at 12 months	No ischemic lesions could be found on the first scan, but 3 patients developed lesions after the cooling period. ADC values correlated significantly with body temperature.

(*continued on next page*)

Table 2 (*continued*)

Source	Study design	n	Region of Interest	Median time ROSC-Scan	Cut off-value	Sens (95% CI)	Spec (95%CI)	Definition poor outcome	Main results
fMRI									
Koenig et al. [71]	Prospective	17		3 days	–	–	–	CPC 3–5 at discharge	Patients had significantly lower connectivity strengths in the default mode network. Furthermore, connectivity strength in the posterior cingulate cortex and the precuneus was greater in patients with good outcome than in patients with poor outcome.
Norton et al. [72]	Prospective	13		3.2 days	–	–	–	Non-reversible coma at 3 months	A present and intact default mode network was observed in controls and those patients with good outcome, but was disrupted in all patients precluding cerebral recovery.
Sair et al. [61]	Prospective	46		12.6 days	–	–	–	CPC 3–5 at 12 months	Patients with a favourable outcome showed higher within connectivity in the default mode network and greater anti-correlation between multiple other resting state networks compared to patients with poor outcome. The network approach discriminated better than DWI and FLAIR measures.
Achard et al. [73]	Prospective	12[c]		"a few days"	–	–	–	–	Global graph based network properties where preserved in comatose patients. A radical reorganization was however found in comatose patients: Cortical regions that were hubs of healthy brain networks had typically become non-hubs of comatose brain networks and vice versa.
DTI									
Iuyt et al. [74]	Prospective	57	Cerebral WM	11 days	FA selective score > 0.44	94 (83–99)	100 (63–100)	GOS-E 1–4 at 12 months	A preliminary prognostic model based on fractional anisotropy values in selected white matter tracts seem to predict 1 year outcome. (WM tracks included in the FA selective score: anterior limb of the left internal capsule, the genu of the corpus callosum and the body of the corpus callosum)
Laitio et al. [75]	Prospective	110	Cerebral WM	53 h	–	–	–	Death at 6 months	Patients who did not survive the 6 months follow-up displayed significantly lower fractional anisotropy than the survivors. Treatment with Xenon gas caused no effect on CPC scores or MRs at 6 months.
Song et al. [76]	Prospective	49	Brainstem, cerebral peduncles, corpus callosum and cerebral hemispheres	11 days	–	–	–	All patients had GOS 1–3 at 12 months (poor outcome)	Cardiac arrest patient show a marked decrease in axial diffusivity in the central regions and cerebral

(*continued on next page*)

Table 2 (*continued*)

Source	Study design	n	Region of Interest	Median time ROSC-Scan	Cut off-value	Sens (95% CI)	Spec (95%CI)	Definition poor outcome	Main results
									hemispheres compared to healthy controls.
Velly et al. [62]	Prospective	200	Whole brain	13 days	WWM-FA < 0.91	89.7 (75.8–97.1)	100 (69.1–100)	Best achieved CPC score of 3–5 in the first 6 months.	Whole brain white matter fractional anisotropy could predict poor outcome in patients who are unconscious 7 days after cardiac arrest.

N = Number of included PAE patients, VS: Vegetative state, CPC: Cerebral Performance Category, DC-LADCV: relative volume of most dominant cluster of ADC values, GOS: Glasgow outcome scale, MRs: Modified Ranking scale, CA: Cardiac arrest, DC-LADCV: Relative volume of most dominant cluster of low-ADC voxels, HCs Healthy controls, Rs: resting state, WM: White matter, WWM-FA: whole brain white matter fractional anisotropy, Confidence intervals are only displayed if mentioned by the authors.

[a] AI these studies qualitatively described differences on group level, mostly without defining the predictive value for an individual patient. Therefore, these studies are grouped within this table.

[b] The "cortex score" consisted of the scores of DWI and/or FLAIR abnormalities in the cortical grey matter of the frontal, parietal, occipital, and temporal lobes, the insular cortex, and the hippocampus. The "deep grey nuclei score" consisted of the scores of the DWI and/or FLAIR abnormality scores of the putamen, globus pallidus, caudate nucleus, and the thalamus. The "cortex plus deep grey nuclei score" combined the cortex score and deep grey nuclei score. The "whole brain" score included all brain regions.

[c] Total of 17 patients, of which 12 after cardiac arrest.

(AUC = 0.88) [61]. Prognostic values for individual patients were not reported.

Graph theory measures divide the brain in a network of nodes and edges. Strongly connected areas are called hub nodes. A single prospective study (n = 12) reported a radical redistribution of hub nodes in comatose patients within a few days after cardiac arrest, compared to healthy controls [73]. Prognostic values for individual patients were not reported.

DTI

Four studies investigated comatose patients after cardiac arrest with DTI (n = 49–200) [62,74–76]. One study found significantly lower fractional anisotropy 15–17 days after cardiac arrest in patients with poor outcome than in patients with good outcome and healthy controls [74]. Differences were most pronounced in the corpus callosum and internal capsule [74]. The established "FA selected" score > 0.44 predicted poor outcome with 100% specificity (CI 63–100%) and a sensitivity of 94% (CI 83–99%) [74]. The corpus callosum and internal capsule were included in this FA-selected score. In patients who remained comatose for at least 7 days after resuscitation, the whole brain white matter fractional anisotropy < 0.91 predicted poor outcome with a 100% specificity and 90% sensitivity according to a second study [62].

In a clinical trial (n = 110) focussing on xenon gas as a therapeutic intervention, patients who died within 6 months after cardiac arrest had significantly lower fractional anisotropy than survivors [75]. A fourth study showed lower diffusivity along the white matter tracts and higher diffusivity perpendicular to the white matter tracts in patients than in healthy controls [76], indicative of axonal damage in the hypoxic-ischemic brain [76,77].

Positron emission tomography

We included 2 small studies using PET analysis for prognostication of hypoxic ischemic brain injury (n = 6–8) [78,79]. One prospective study found a decreased glucose consumption in both white and grey matter of patients one day post resuscitation [78]. None of the 8 investigated subjects had a good outcome and only two patients survived longer than two weeks after cardiac arrest. Glucose consumption was significantly decreased in all brain regions compared to healthy controls. No differences in glucose consumptions were found between survivors and non-survivors. Cerebral perfusion was comparable between patients and controls.

A second PET study found a reduced cerebral oxygen metabolism ($CMRO_2$) to 30% of normal, measured more than one week after cardiac arrest to be a sign for prolonged, but not necessarily persistent coma [79]. Reduced $CMRO_2$ in unconscious patients might have been related to sedation effects, because all patients were mechanically ventilated during PET scanning. After 7 days a decreased oxygen extraction fraction became distinctive between patients with good and poor outcome. No reliable prognosticator could be established from this study, because of the small sample size (n = 6) and because all patients died as a result of recurrent myocardial infarctions.

Discussion

We reviewed the value of imaging techniques to assist in neurological prognostication of comatose patients with hypoxic-ischemic brain injury. The most studied parameters, decreased GWR based on CT and ADC values as measured by MRI, are based on cytotoxic oedema. GWR values lower than 1.10 and ADC values lower than 650 $*10^{-6}$ mm^2/s in at least 10% of the brain repeatedly predicted poor outcome with a 100% specificity but at a highly variable sensitivity. Predictive values of the GWR were high from the first hour to 3 days after cardiac arrest. The optimal time window for prognostication based on ADC was between two and five days after resuscitation. Semi-quantification of

Table 3
PET parameters and their prognostic value.

Source	Study design	n	Region of Interest	Median time ROSC-Scan	Cut off-value	Sens (%)	Spec %	Definition poor outcome	Main results
Schaafsma et al. [78]	Prospective	8	Whole brain	Day 1	–	–	–	All patients had poor outcome (GOS 1–2)	All patients in this study had a poor outcome. The investigated PET measures showed no differences between survivors and non-survivors. Glucose consumption was significantly decreased in all patients, compared to healthy controls.
Edgren et al. [79]	Prospective	6	Whole brain	Day 1, 3 & 7	–	–	–	Remain comatose > 4 days after resuscitation	All patients showed initial low cerebral oxygen metabolism ($CMRO_2$). When the $CMRO_2$ was low > 1week, this was a sign for prolonged coma.

GOS: Glasgow outcome scale.

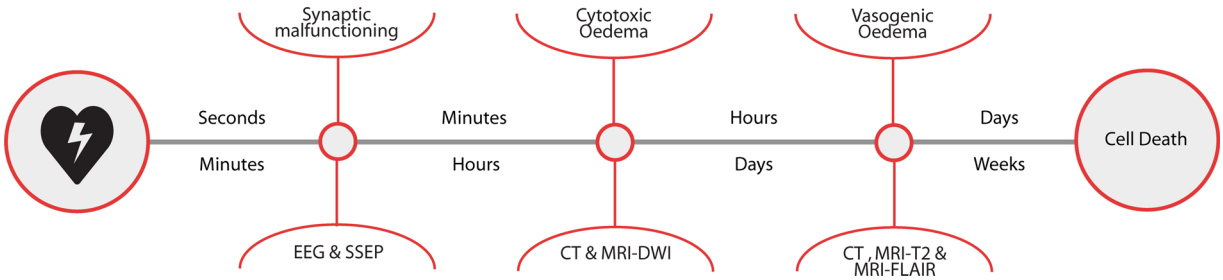

Fig. 1. Timeline of neuronal damage after cardiac arrest and diagnostic measures sensitive to detection of abnormalities for each phase. DTI and fMRI are missing in this figure, because of inconclusive evidence about the optimal timing.

visual DWI and FLAIR interpretation reliably predicted poor outcome with moderate to high sensitivities of 40–100% [34,36,62]. Only one study included in this review gave a detailed description of the spatiotemporal pattern of abnormalities after hypoxic-ischemic brain injury, based on MRI [55]. They found abnormalities in the cerebral cortex, the putamen and cerebellum to be most distinctive between patients with good and poor outcome in the first 2–3 days after cardiac arrest. Other studies also report the cortical structures and the deep grey matter to be most sensitive for hypoxic damage [21,22,34,36].

Since multiple studies report high predictive values, GWR and ADC probably contain valuable information for poor outcome prediction.

All relevant CT parameters and DWI measures are based on cytotoxic oedema. Apparently, substantial cytotoxic oedema precludes relevant recovery. Since not all patients with poor recovery show cytotoxic oedema, measures of cytotoxic oedema may be complementary to other factors that predict poor outcome, such as synaptic failure (EEG) or disruption of connectivity (fMRI or DTI). Presence of vasogenic oedema seems to have limited additional predictive value.

DTI and fMRI are promising with regard to additive value for prognostication of outcome after cardiac arrest. On a group level, differences in connection strengths in the default mode network between patients with poor and good outcome have been found approximately 3 days after cardiac arrest. Two studies found high prognostic values of DTI performed approximately 2 weeks after cardiac arrest (spec 100%, sens. 90–94%) [62,74]. Since EEG differences between patients with good and poor outcome are largest within the first 24 h, discrimination of fMRI may be enhanced by earlier scanning.

In almost all studies that investigated CT and MRI, scans were performed in patients who had been treated with 24 h of therapeutic hypothermia (32–34 °C). In these studies, patients were scanned before, during or after application of hypothermia. At all time-points, differences between patients with favourable and unfavourable outcome were found. The use of hypothermia may influence the spatiotemporal pattern of brain damage, and ADC values are known to be influenced by temperature [80]. However, the exact effects of temperature remain unclear.

Techniques that rely on functionality of the brain, such as fMRI and PET, are likely to be affected by sedation effects. One study using fMRI added sedation as a covariate in their prediction model and found that sedation indeed has an effect on the measurements [71]. When the level of sedation was added as a covariate in the prediction model, subjects with poor outcome showed even lower connectivity strengths than those with good outcome [71].

Quantitative MRI techniques, such as ADC maps, fMRI, or diffusion tensors, are sensitive to differences in imaging setup [81–85]. Also, the MRI vendor and available packages influence measurements. Although

Fig. 2. Example of an adults non-contrast brain CT-scan following cardiac arrest. Especially the occipital regions are affected in this case, showing diffuse swelling and sulcal effacement. Distinction between grey and white matter (the 'grey-white matter ratio') is diminished throughout the brain.

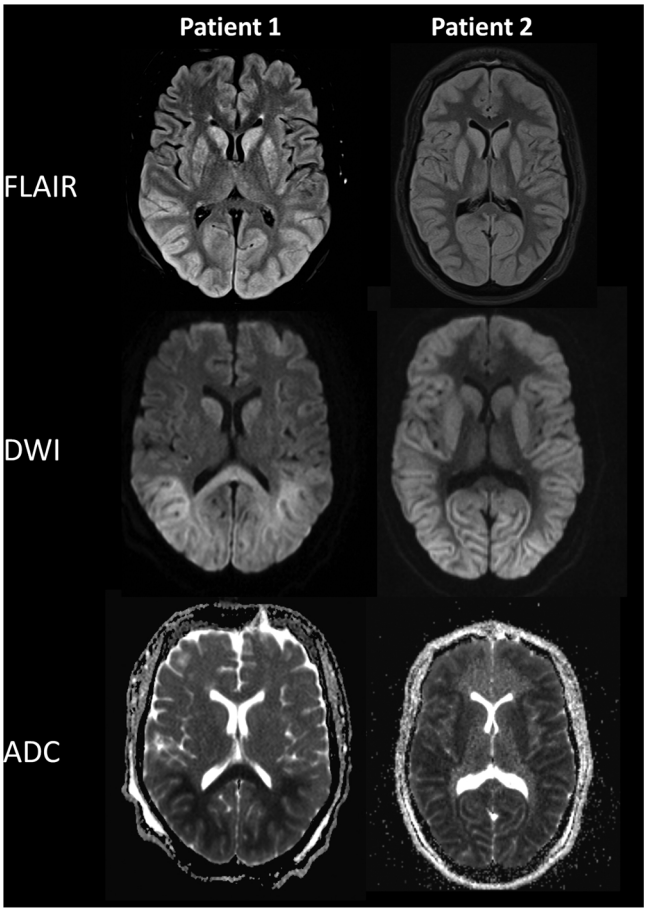

Fig. 3. FLAIR, DWI and ADC images of 2 adult patients following cardiac arrest. Patient 1 shows FLAIR signal hyperintensities, diffusion and mass effects in the posterior parts of the brain on the second day after the event. The deep grey nuclei are also affected, but show less diffusion restriction. A second scan made 14 days after the event showed no diffusion restriction, while parenchymal gliosis could be seen on T2 imaging (figures not included). Patient 2 shows FLAIR signal hyperintensities, mass effects and diffusion restriction in all grey matter structures. This is an example of very severe global hypoxic brain damage.

differences between scanners often remain within the 2SD interval, variability in MR measures in different settings complicates the possibility to establish a reliable threshold for prediction of poor neurologic prognosis. It is therefore crucial to harmonize imaging protocols between sites when performing multicentre studies, to re-evaluate imaging protocols after system updates, and to provide a detailed description of the protocols for imaging and analysis. Visual analysis of MRI scans is less influenced by MRI vendor.

This is a narrative review, without a systematic analysis of the quality of the included studies and resulting evidence according to the PRISMA guidelines. Therefore, our appreciation of the evidence is largely qualitative. Based on the diversity of study designs, preventing the possibility of any meta-analysis, unblinded outcome assessments with risk of bias, limited numbers of inclusions with wide confidence intervals, divergent, retrospectively adjudicated cut off values, and lack of external validation, we conclude that the current evidence for CT or MRI measures for reliable prediction of poor outcome of comatose patients after cardiac arrest is weak

A perfect model for prognostication of comatose patients after cardiac arrest does not exist. GWR $<$ 1.10 on a CT-scan made within 24 h after cardiac arrest is strongly associated with poor outcome, but not 100% specific. Between day 2 and 5 after resuscitation, ADC $<$ 650 $\times$ 10-6 mm^2/ s in 22% of the brain volume points towards permanent brain damage, but does not preclude functional recovery. The prognostic value of brain imaging therefore remains insufficient to use as a single predictor of cerebral recovery.

We recommend to perform future imaging studies in a multimodal setting, combining imaging techniques with other potential predictors. This will allow establishment of the *additional* prognostic value of imaging techniques, as well as combining multiple methods into prediction models. We further recommend strict acknowledgement of timing of imaging with regard to cardiac arrest, since changes on CT and MRI are highly dynamic. Furthermore, exploration of fMRI, DTI and automated image processing may contribute to optimization of prediction models.

Conclusion

CT and MRI studies have shown significant differences between comatose patients after cardiac arrest with favourable and unfavourable outcome. These differences represent various pathophysiological mechanisms following global anoxia of the brain. GWR may indicate poor outcome in the first hours to days after cardiac arrest, while ADC measurements may be predictive after 2–5 days. However, prospective multicentre studies with sufficiently large sample sizes are needed to determine whether specific imaging parameters or spatiotemporal patterns of abnormalities, when added to clinical signs, SSEP and EEG, further enhance prediction of outcome of comatose patients after cardiac arrest in an early phase.

Conflict of interests

None.

Acknowledgment

H. Keijzer is funded by the Rijnstate-Radboudumc promotion fund.

References

[1] Neumar RW, Nolan JP, Adrie C, Aibiki M, Berg RA, Bottiger BW, et al. Post-cardiac arrest syndrome: epidemiology, pathophysiology, treatment, and prognostication. A consensus statement from the International Liaison Committee on Resuscitation (American Heart Association, Australian and New Zealand Council on Resuscitation, European Resuscitation Council, Heart and Stroke Foundation of Canada, InterAmerican Heart Foundation, Resuscitation Council of Asia, and the Resuscitation Council of Southern Africa); the American Heart Association Emergency Cardiovascular Care Committee; the Council on Cardiovascular Surgery and Anesthesia; the Council on Cardiopulmonary, Perioperative, and Critical Care; the Council on Clinical Cardiology; and the Stroke Council. Circulation 2008;118(23):2452–83.
[2] Hofmeijer J, Beernink TMJ, Bosch FH, Beishuizen A, Tjepkema-Cloostermans MC, van Putten MJAM. Early EEG contributes to multimodal outcome prediction of postanoxic coma. Neurology 2015;85(2):137–43.
[3] Tiainen M, Poutiainen E, Kovala T, Takkunen O, Happola O, Roine RO. Cognitive and neurophysiological outcome of cardiac arrest survivors treated with therapeutic hypothermia. Stroke J Cereb Circ 2007;38.
[4] Nielsen N, Wetterslev J, Cronberg T, Erlinge D, Gasche Y, Hassager C, et al. Targeted temperature management at 33°C versus 36°C after cardiac arrest. N Engl J Med 2013;369(23):2197–206.
[5] Rossetti AO, Rabinstein AA, Oddo M. Neurological prognostication of outcome in patients in coma after cardiac arrest. Lancet Neurol 2016;15(6):597–609.
[6] Stroke: national clinical guideline for diagnosis and initial management of acute stroke and Transient Ischaemic Attack (TIA). London: Royal College of Physicians; 2008.
[7] Friberg H, Cronberg T, Dünser MW, Duranteau J, Horn J, Oddo M. Survey on current practices for neurological prognostication after cardiac arrest. Resuscitation 2015;90:158–62.
[8] Greer DM, Rosenthal ES, Wu O. Neuroprognostication of hypoxic-ischaemic coma in the therapeutic hypothermia era. Nat Rev Neurol 2014;10(4):190–203.
[9] Nolan JP, Soar J, Cariou A, Cronberg T, Moulaert VR, Deakin CD, et al. European Resuscitation Council and European Society of Intensive Care Medicine Guidelines for post-resuscitation care 2015: section 5 of the European Resuscitation Council Guidelines for Resuscitation 2015. Resuscitation 2015;95:202–22.
[10] Sandroni C, Cariou A, Cavallaro F, Cronberg T, Friberg H, Hoedemaekers C, et al. Prognostication in comatose survivors of cardiac arrest: an advisory statement from the European Resuscitation Council and the European Society of Intensive Care Medicine. Intens Care Med 2014;40(12):1816–31.
[11] Cloostermans MC, van Meulen FB, Eertman CJ, Hom HW, van Putten MJAM.

Continuous electroencephalography monitoring for early prediction of neurological outcome in postanoxic patients after cardiac arrest: a prospective cohort study. Crit Care Med 2012;40(10):2867–75.
[12] Attwell D, Laughlin SB. An energy budget for signaling in the grey matter of the brain. J Cereb Blood Flow Metab 2001;21(10):1133–45.
[13] Harris JJ, Jolivet R, Attwell D. Synaptic energy use and supply. Neuron 2012;75(5):762–77.
[14] Murphy TH, Corbett D. Plasticity during stroke recovery: from synapse to behaviour. Nat Rev Neurosci 2009;10(12):861–72.
[15] Buunk G, van der Hoeven JG, Meinders AE. Cerebral blood flow after cardiac arrest. Neth J Med 2000;57(3):106–12.
[16] Hofmeijer J, van Putten MJ. Ischemic cerebral damage: an appraisal of synaptic failure. Stroke 2012;43(2):607–15.
[17] Bolay H, Gursoy-Ozdemir Y, Sara Y, Onur R, Can A, Dalkara T. Persistent defect in transmitter release and synapsin phosphorylation in cerebral cortex after transient moderate ischemic injury. Stroke 2002;33(5):1369–75.
[18] Bandera E, Botteri M, Minelli C, Sutton A, Abrams KR, Latronico N. Cerebral blood flow threshold of ischemic penumbra and infarct core in acute ischemic stroke: a systematic review. Stroke 2006;37(5):1334–9.
[19] Dijkstra K, Hofmeijer J, van Gils SA, van Putten MJ. A biophysical model for cytotoxic cell swelling. J Neurosci 2016;36(47):11881–90.
[20] von Kummer R, Dzialowski I. Imaging of cerebral ischemic edema and neuronal death. Neuroradiology 2017;59(6):545–53.
[21] Busl KM, Greer DM. Hypoxic-ischemic brain injury: pathophysiology, neuropathology and mechanisms. NeuroRehabilitation 2010;26(1):5–13.
[22] Gutierrez LG, Rovira À, Portela LAP, Leite CdC, Lucato LT. CT and MR in non-neonatal hypoxic–ischemic encephalopathy: radiological findings with pathophysiological correlations. Neuroradiology 2010;52(11):949–76.
[23] Tjepkema-Cloostermans MC, Hindriks R, Hofmeijer J, van Putten MJ. Generalized periodic discharges after acute cerebral ischemia: reflection of selective synaptic failure? Clin Neurophysiol 2014;125(2):255–62.
[24] Ruijter BJ, van Putten MJ, Hofmeijer J. Generalized epileptiform discharges in postanoxic encephalopathy: quantitative characterization in relation to outcome. Epilepsia 2015;56(11):1845–54.
[25] Kimberly HH, Shah S, Marill K, Noble V. Correlation of optic nerve sheath diameter with direct measurement of intracranial pressure. Acad Emerg Med 2008;15(2):201–4.
[26] Chae MK, Ko E, Lee JH, Lee TR, Yoon H, Hwang SY, et al. Better prognostic value with combined optic nerve sheath diameter and grey-to-white matter ratio on initial brain computed tomography in post-cardiac arrest patients. Resuscitation 2016;104:40–5.
[27] Cristia C, Ho ML, Levy S, Andersen LW, Perman SM, Giberson T, et al. The association between a quantitative computed tomography (CT) measurement of cerebral edema and outcomes in post-cardiac arrest-a validation study. Resuscitation 2014;85(10):1348–53.
[28] Gentsch A, Storm C, Leithner C, Schroeder T, Ploner CJ, Hamm B, et al. Outcome prediction in patients after cardiac arrest: a simplified method for determination of gray-white matter ratio in cranial computed tomography. Clin Neuroradiol 2015;25(1):49–54.
[29] Inamasu J, Miyatake S, Suzuki M, Nakatsukasa M, Tomioka H, Honda M, et al. Early CT signs in out-of-hospital cardiac arrest survivors: temporal profile and prognostic significance. Resuscitation 2010;81(5):534–8.
[30] Yamamura H, Kaga S, Kaneda K, Yamamoto T, Mizobata Y. Head Computed Tomographic measurement as an early predictor of outcome in hypoxic-ischemic brain damage patients treated with hypothermia therapy. Scand J Trauma Resusc Emerg Med 2013;21(37).
[31] Lee BK, Kim YJ, Ryoo SM, Kim SJ, Lee DH, Jeung KW, et al. "Pseudo-subarachnoid hemorrhage sign" on early brain computed tomography in out-of-hospital cardiac arrest survivors receiving targeted temperature management. J Crit Care 2017;40:36–40.
[32] Yuzawa H, Higano S, Mugikura S, Umetsu A, Murata T, Nakagawa A, et al. Pseudo-subarachnoid hemorrhage found in patients with postresuscitation encephalopathy: characteristics of CT findings and clinical importance. AJNR Am J Neuroradiol 2008;29(8):1544–9.
[33] Wijdicks EF, Campeau NG, Miller GM. MR imaging in comatose survivors of cardiac resuscitation. AJNR Am J Neuroradiol 2001;22(8):1561–5.
[34] Park JS, Lee SW, Kim H, Min JH, Kang JH, Yi KS, et al. Efficacy of diffusion-weighted magnetic resonance imaging performed before therapeutic hypothermia in predicting clinical outcome in comatose cardiopulmonary arrest survivors. Resuscitation 2015;88:132–7.
[35] Howard RS, Holmes PA, Siddiqui A, Treacher D, Tsiropoulos I, Koutroumanidis M. Hypoxic-ischaemic brain injury: imaging and neurophysiology abnormalities related to outcome. QJM 2012;105(6):551–61.
[36] Hirsch KG, Mlynash M, Jansen S, Persoon S, Eyngorn I, Krasnokutsky MV, et al. Prognostic value of a qualitative brain MRI scoring system after cardiac arrest. J Neuroimaging 2015;25(3):430–7.
[37] Helenius J, Soinne L, Perkiö J, Salonen O, Kangasmäki A, Kaste M, et al. Diffusion-weighted MR imaging in normal human brains in various age groups. Am J Neuroradiol 2002;23(2):194–9.
[38] Heine L, Soddu A, Gomez F, Vanhaudenhuyse A, Tshibanda L, Thonnard M, et al. Resting state networks and consciousness: alterations of multiple resting state network connectivity in physiological, pharmacological, and pathological consciousness states. Front Psychol 2012;3:295.
[39] Yanagawa Y, Un-no Y, Sakamoto T, Okada Y. Cerebral density on CT immediately after a successful resuscitation of cardiopulmonary arrest correlates with outcome. Resuscitation 2005;64(1):97–101.
[40] Metter RB, Rittenberger JC, Guyette FX, Callaway CW. Association between a quantitative CT scan measure of brain edema and outcome after cardiac arrest. Resuscitation 2011;82(9):1180–5.
[41] Lee BK, Kim WY, Shin J, Oh JS, Wee JH, Cha KC, et al. Prognostic value of gray matter to white matter ratio in hypoxic and non-hypoxic cardiac arrest with non-cardiac etiology. Am J Emerg Med 2016;34(8):1583–8.
[42] Hwan Kim Y, Ho Lee J, Kun Hong C, Won Cho K, Hoon Yeo J, Ju Kang M, et al. Feasibility of optic nerve sheath diameter measured on initial brain computed tomography as an early neurologic outcome predictor after cardiac arrest. Acad Emerg Med 2014;21(10):1121–8.
[43] Scheel M, Storm C, Gentsch A, Nee J, Luckenbach F, Ploner CJ, et al. The prognostic value of gray-white-matter ratio in cardiac arrest patients treated with hypothermia. Scand J Trauma Resusc Emerg Med 2013;21(23).
[44] Lee BK, Jeung KW, Lee HY, Jung YH, Lee DH. Combining brain computed tomography and serum neuron specific enolase improves the prognostic performance compared to either alone in comatose cardiac arrest survivors treated with therapeutic hypothermia. Resuscitation 2013;84(10):1387–92.
[45] Torbey MT, Selim M, Knorr J, Bigelow C, Recht L. Quantitative analysis of the loss of distinction between gray and white matter in comatose patients after cardiac arrest. Stroke 2000;31(9):2163–7.
[46] Wu O, Batista LM, Lima FO, Vangel MG, Furie KL, Greer DM. Predicting clinical outcome in comatose cardiac arrest patients using early noncontrast computed tomography. Stroke 2011;42(4):985–92.
[47] Sahutoglu C, Uyar M, Demirag K, Isayev H, Moral AR. Predictive value of brain arrest neurological outcome scale (BrANOS) on mortality and morbidity after cardiac arrest. Turk J Anaesthesiol Reanim 2016;44(6):295–300.
[48] Scarpino M, Lanzo G, Lolli F, Carrai R, Moretti M, Spalletti M, et al. Neurophysiological and neuroradiological multimodal approach for early poor outcome prediction after cardiac arrest. Resuscitation 2018;129:114–20.
[49] Youn CS, Callaway CW, Rittenberger JC, Post Cardiac Arrest S. Combination of initial neurologic examination, quantitative brain imaging and electroencephalography to predict outcome after cardiac arrest. Resuscitation 2017;110:120–5.
[50] Jeon CH, Park JS, Lee JH, Kim H, Kim SC, Park KH, et al. Comparison of brain computed tomography and diffusion-weighted magnetic resonance imaging to predict early neurologic outcome before target temperature management comatose cardiac arrest survivors. Resuscitation 2017;118:21–6.
[51] Lee BK, Jeung KW, Song KH, Jung YH, Choi WJ, Kim SH, et al. Prognostic values of gray matter to white matter ratios on early brain computed tomography in adult comatose patients after out-of-hospital cardiac arrest of cardiac etiology. Resuscitation 2015;96:46–52.
[52] Choi SP, Park HK, Park KN, Kim YM, Ahn KJ, Choi KH, et al. The density ratio of grey to white matter on computed tomography as an early predictor of vegetative state or death after cardiac arrest. Emerg Med J 2008;25(10):666–9.
[53] Torbey MT, Geocadin R, Bhardwaj A. Brain arrest neurological outcome scale (BrANOS): predicting mortality and severe disability following cardiac arrest. Resuscitation 2004;63(1):55–63.
[54] Moseby-Knappe M, Pellis T, Dragancea I, Friberg H, Nielsen N, Horn J, et al. Head computed tomography for prognostication of poor outcome in comatose patients after cardiac arrest and targeted temperature management. Resuscitation 2017;119:89–94.
[55] Mlynash M, Campbell DM, Leproust EM, Fischbein NJ, Bammer R, Eyngorn I, et al. Temporal and spatial profile of brain diffusion-weighted MRI after cardiac arrest. Stroke 2010;41(8):1665–72.
[56] Ryoo SM, Jeon SB, Sohn CH, Ahn S, Han C, Lee BK, et al. Predicting outcome with diffusion-weighted imaging in cardiac arrest patients receiving hypothermia therapy: multicenter retrospective cohort study. Crit Care Med 2015;43(11):2370–7.
[57] Youn CS, Park KN, Kim JY, Callaway CW, Choi SP, Rittenberger JC, et al. Repeated diffusion weighted imaging in comatose cardiac arrest patients with therapeutic hypothermia. Resuscitation 2015;96:1–8.
[58] Leao RN, Avila P, Cavaco R, Germano N, Bento L. Therapeutic hypothermia after cardiac arrest: outcome predictors. Rev Bras Ter Intensiva 2015;27(4):322–32.
[59] Greer D, Scripko P, Bartscher J, Sims J, Camargo E, Singhal A, et al. Clinical MRI interpretation for outcome prediction in cardiac arrest. Neurocrit Care 2012;17(2):240–4.
[60] Topcuoglu MA, Oguz KK, Buyukserbetci G, Bulut E. Prognostic value of magnetic resonance imaging in post-resuscitation encephalopathy. Intern Med 2009;48(18):1635–45.
[61] Sair HI, Hannawi Y, Li S, Kornbluth J, Demertzi A, Di Perri C, et al. Early functional connectome integrity and 1-year recovery in comatose survivors of cardiac arrest. Radiology 2017:162161.
[62] Velly L, Perlbarg V, Boulier T, Adam N, Delphine S, Luyt C-E, et al. Use of brain diffusion tensor imaging for the prediction of long-term neurological outcomes in patients after cardiac arrest: a multicentre, international, prospective, observational, cohort study. Lancet Neurol 2018;17(4):317–26.
[63] Hirsch KG, Mlynash M, Eyngorn I, Pirsaheli R, Okada A, Komshian S, et al. Multicenter study of diffusion-weighted imaging in coma after cardiac arrest. Neurocrit Care 2016;24(1):82–9.
[64] Kim J, Kim K, Suh GJ, Kwon WY, Kim KS, Shin J, et al. Prognostication of cardiac arrest survivors using low apparent diffusion coefficient cluster volume. Resuscitation 2016;100:18–24.
[65] Wijman CA, Mlynash M, Caulfield AF, Hsia AW, Eyngorn I, Bammer R, et al. Prognostic value of brain diffusion-weighted imaging after cardiac arrest. Ann Neurol 2009;65(4):394–402.
[66] Wu O, Sorensen AG, Benner T, Singhal AB, Furie KL, Greer DM. Comatose patients with cardiac arrest: predicting clinical outcome with diffusion-weighted MR imaging. Radiology 2009;252(1):173–81.
[67] Heradstveit BE, Larsson EM, Skeidsvoll H, Hammersborg SM, Wentzel-Larsen T, Guttormsen AB, et al. Repeated magnetic resonance imaging and cerebral

performance after cardiac arrest–a pilot study. Resuscitation 2011;82(5):549–55.
[68] Kim J, Choi BS, Kim K, Jung C, Lee JH, Jo YH, et al. Prognostic performance of diffusion-weighted MRI combined with NSE in comatose cardiac arrest survivors treated with mild hypothermia. Neurocrit Care 2012;17(3):412–20.
[69] Choi S, Park K, Park H, Kim J, Youn C, Ahn K, et al. Diffusion-weighted magnetic resonance imaging for predicting the clinical outcome of comatose survivors after cardiac arrest: a cohort study. Crit Care 2010;14(1):R17.
[70] Mettenburg JM, Agarwal V, Baldwin M, Rittenberger JC. Discordant observation of brain injury by MRI and malignant electroencephalography patterns in comatose survivors of cardiac arrest following therapeutic hypothermia. AJNR Am J Neuroradiol 2016;37(10):1787–93.
[71] Koenig MA, Holt JL, Ernst T, Buchthal SD, Nakagawa K, Stenger VA, et al. MRI default mode network connectivity is associated with functional outcome after cardiopulmonary arrest. Neurocrit Care 2014;20(3):348–57.
[72] Norton L, Hutchison RM, Young GB, Lee DH, Sharpe MD, Mirsattari SM. Disruptions of functional connectivity in the default mode network of comatose patients. Neurology 2012;78(3):175–81.
[73] Achard S, Delon-Martin C, Vertes PE, Renard F, Schenck M, Schneider F, et al. Hubs of brain functional networks are radically reorganized in comatose patients. Proc Natl Acad Sci U S A 2012;109(50):20608–13.
[74] luyt C, Galanaud D, Perlbarg V, vanhaudenhuyse A, Stevens RD, Gupta R, et al. Diffusion tensor imaging to predict long-term outcome after cardiac arrest - a bi-centric pilot study. Anesthesiology 2012;117(6).
[75] Laitio R, Hynninen M, Arola O, Virtanen S, Parkkola R, Saunavaara J, et al. Effect of inhaled xenon on cerebral white matter damage in comatose survivors of out-of-hospital cardiac arrest: a randomized clinical trial. JAMA 2016;315(11):1120–8.
[76] van der Eerden AW, Khalilzadeh O, Perlbarg V, Dinkel J, Sanchez P, Vos PE, et al. White matter changes in comatose survivors of anoxic ischemic encephalopathy and traumatic brain injury: comparative diffusion-tensor imaging study. Neuroradiology 2014;270(2).
[77] Song S-K, Sun S-W, Ju W-K, Lin S-J, Cross AH, Neufeld AH. Diffusion tensor imaging detects and differentiates axon and myelin degeneration in mouse optic nerve after retinal ischemia. NeuroImage 2003;20(3):1714–22.
[78] Schaafsma A, de Jong BM, Bams JL, Haaxma-Reiche H, Pruim J, Zijlstra JG. Cerebral perfusion and metabolism in resuscitated patients with severe post-hypoxic encephalopathy. J Neurol Sci 2003;210(1-2):23–30.
[79] Edgren E, Enblad P, Grenvik Å, Lilja A, Valind S, Wiklund L, et al. Cerebral blood flow and metabolism after cardiopulmonary resuscitation. A pathophysiologic and prognostic positron emission tomography pilot study. Resuscitation 2003;57(2):161–70.
[80] Yenari MA, Onley D, Hedehus M, deCrespigny A, Sun GH, Moseley ME, et al. Diffusion- and perfusion-weighted magnetic resonance imaging of focal cerebral ischemia and cortical spreading depression under conditions of mild hypothermia. Brain Res 2000;885(2):208–19.
[81] Jovicich J, Marizzoni M, Sala-Llonch R, Bosch B, Bartres-Faz D, Arnold J, et al. Brain morphometry reproducibility in multi-center 3T MRI studies: a comparison of cross-sectional and longitudinal segmentations. Neuroimage 2013;83:472–84.
[82] Mutsaerts HJ, Steketee RM, Heijtel DF, Kuijer JP, van Osch MJ, Majoie CB, et al. Inter-vendor reproducibility of pseudo-continuous arterial spin labeling at 3 Tesla. PLoS One 2014;9(8):e104108.
[83] Wang ZJ, Seo Y, Babcock E, Huang H, Bluml S, Wisnowski J, et al. Assessment of diffusion tensor image quality across sites and vendors using the American College of Radiology head phantom. J Appl Clin Med Phys 2016;17(3):442–51.
[84] Magnotta VA, Matsui JT, Liu D, Johnson HJ, Long JD, Bolster Jr. BD, et al. Multicenter reliability of diffusion tensor imaging. Brain Connect 2012;2(6):345–55.
[85] Marchitelli R, Minati L, Marizzoni M, Bosch B, Bartres-Faz D, Muller BW, et al. Test-retest reliability of the default mode network in a multi-centric fMRI study of healthy elderly: effects of data-driven physiological noise correction techniques. Hum Brain Mapp 2016;37(6):2114–32.
[86] Els T, Kassubek J, Kubalek R, Klisch J. Diffusion-weighted MRI during early global cerebral hypoxia: a predictor for clinical outcome? Acta Neurol Scand 2004;110(6):361–7.